5

Magnetic Relaxation - Methods for Stabilization of Magnetization and Levitation Force

Boris Smolyak, Maksim Zakharov and German Ermakov
Institute of Thermal Physics Ural Branch of RAS
Russian Federation

1. Introduction

Bulk high-temperature superconductors (HTS) are used as current-carrying elements in various devices: electrical machines, magnetic suspension systems, strong magnetic field sources, etc. Supercurrents decay due to the relaxation of nonequilibrium magnetic structures. This phenomenon, which is known as magnetic flux creep or magnetic relaxation, degrades the characteristics of superconducting devices. A "giant flux creep" is observed in HTS. There is an extensive review on this phenomenon by Yeshurun et al. (1996), but the magnetic relaxation suppression was discussed only briefly in it. An overwhelming majority of studies dealing with applications of HTS also paid little attention to the problem of creep. In this chapter we describe the methods of influence on the relaxation rate both of local characteristics of the magnetic structure (vortex density and vortex density gradient) and averages over the volume of superconductor (magnetic flux, magnetic moment and levitation force). Particular emphasis is placed on the magnetization and the magnetic force whose stability is necessary for the normal operation of the majority of high-current superconducting devices.

Magnetic flux creep has its origin in motion vortex (flux lines) out of their pinning sites due to the thermal activation. The creep rate decreases when new or denser pinning sites are introduced into HTS sample. The overview of different techniques for producing pinning sites may be found in the review by Yeshurun et al. (1996). The dramatic decrease in the magnetic relaxation rate is observed if the temperature of the superconductor is reduced (Maley et al., 1990; Sun et al., 1990; Thompson et al., 1991). This effect known as "flux annealing" arises due to the transition of vortex system from the critical state having small activation energy to the subcritical state with relatively large activation energy. The "flux annealing" suppresses flux creep, but does not affect the magnetic structure. The induction gradient, which determines the supercurrent density and the superconductor magnetization, does not change after "annealing". However, this method is difficult to implement in technological applications. On the contrary, the exposure of ac magnetic fields strongly affects the nonequilibrium vortex configuration. The critical state in superconductor is completely destroyed at the certain amplitude of ac field (Fisher et al., 1997; Willemin et al., 1998). If the amplitude is less than it, the induction gradient is destroyed at the depth of ac field penetration (Fisher et at., 1997; Smolyak et al., 2007), and in the region bordering the penetration region gradient structure experiences strong relaxation which is not related to thermal activation (Brandt & Mikitik, 2003). After switching off ac field the remanent stationary magnetization is much smaller, but

it decays with time much slower than before the exposure of ac field. It was found that after the exposure of transverse ac field the remanent induction distribution does not change for a long time, i.e. the subcritical vortex configuration is formed (Fisher et al., 2005; Voloshin et al., 2007). However, the use of ac field to suppress creep in superconducting devices is not effective because the initial magnetization is highly reduced.

A classical paper on the flux creep (Beasly et al., 1969) probably was the first to note that the total magnetic flux in superconductor remains unchanged for a long time after the small reversal of external magnetic field. This effect was studied later in more detail, and it formed the basis of the reverse methods for the stabilization of magnetization (Kwasnitza & Widmer, 1991, 1993) and levitation force (Smolyak et al., 2000, 2002). The reversal leads to the internal magnetic relaxation (Smolyak et al., 2001) when the volume-averaged quantities do not change for a long time. The phenomenon of internal magnetic relaxation is considered in more detail below in the section 3.

Smolyak et al. (2006) studied the dependence of relaxation rate of magnetic force on the rigidity of constraints imposed on a "magnet-superconductor" system. The magnetic force in the suspension system decreases at maximum rate when HTS sample and magnet are rigidly fixed; that is, a rigid mechanical constraint is imposed on the suspension object (HTS sample or magnet). As the mechanical constraint is made weaker, the creep of magnetic force is retarded. The closer the suspension system to the "true" levitation (in which the mobility of the sample is determined predominantly by the magnetoelastic coupling), the slower the magnetic force decays with time. This effect is of great importance for levitation systems and discussed in the section 4.

A new effect has been described recently by Smolyak & Ermakov (2010a, 2010b). It was found that the magnetic relaxation is suppressed in HTS sample with a trapped magnetic flux when the sample approaches a ferromagnet. The local relaxation of induction is absent, too; that is, the flux distribution is rigid and does not vary with time. This effect is considered in the section 5.

2. Magnetization and magnetic force

Let a superconducting disk having a radius R and a thickness d be magnetized as it moves along the z-axis in a nonuniform magnetic field having an azimuthal symmetry (the side surface of the disk is parallel to the z-axis). The disk can perform reverse movements resulting to the azimuthal currents of density J_θ with alternating directions are induced in it. Assume that the critical state extends into the disk from its rim, i.e. the currents induced only by the radial vortex-density gradient:

$$J_\theta = -\frac{1}{\mu_0}\frac{dB_z}{dr}(r), \tag{1}$$

where B_z denotes the axial component of induction and μ_0 is the magnetic constant.

The disk magnetization along the z-axis may be written as:

$$M = \frac{1}{R_2}\int_0^R J_\theta(r) r^2 dr . \tag{2}$$

The force acting upon the disk along the z-axis:

$$F = \int_V J_\theta(r) B_r(r,z)\, d\upsilon\,, \tag{3}$$

where B_r is the radial component of the field induction; V is the disk volume. The density of ponderomotive forces $J_\theta B_r$ depends on the true value of field which is produced both by the external source and the currents influenced by the force. However, when a full force is calculated from Eq. (3), B_r may be assumed to mean the external field only (Landau et al., 1957).

Let us use the Bean's model of critical state according to which the critical current density J_c is constant throughout the volume. In Eq. (1) $J_\theta = J_c$ (if $dB_z/dr < 0$), $J_\theta = -J_c$ (if $dB_z/dr > 0$) and $J_\theta = 0$ (if $dB_z/dr = 0$). The disk will have a maximum magnetization if a unidirectional current flows in the whole volume of the disk ($0 \le r \le R$):

$$M_m = \frac{1}{3} JR \tag{4}$$

The subscript c at J is omitted because the current density decreases with time.

If the current flows in the region $r_1 \le r \le r_2$ ($r_2 < R$), the disk has a partial unipolar magnetization:

$$M = M_m \left(\frac{r_2^3 - r_1^3}{R^3} \right). \tag{5}$$

If the currents producing opposite magnetic moments circulate in the sample, the disk has a bipolar magnetization:

$$M^* = M_m \left[2\left(\frac{r^*}{R} \right)^3 - \left(\frac{r_1}{R} \right)^3 - 1 \right], \tag{6}$$

where r^* is the boundary between regions passing counter currents ($r_1 < r^* < R$); the critical state occupies the region $r_1 \le r \le R$. Here and henceforth the quantities relating to the bipolar current structure are marked with an asterisk (e.g. $F(M^*) \equiv F^*$ etc.).

The magnetic field with azimuthal symmetry is usually created by disk or ring permanent magnets, and in some cases $B_r(r)$ can be approximated by a linear dependence. Then the expression for the force (3) may be written as (Smolyak et al., 2002):

$$F = \Phi_r M\,, \tag{7}$$

$$\Phi_r = 2\pi R \int_z^{z+d} B_r(R,z)\, dz\,, \tag{8}$$

where Φ_r is the radial magnetic flux piercing the disk rim. This flux can also be expressed as the axial induction gradient averaged over the disk volume V:

$$\Phi_r = \left\langle \frac{dB_z}{dz} \right\rangle V\,. \tag{9}$$

If the HTS sample does not move after the magnetization, the magnitude Φ_r in Eq. (7) does not change with time and, consequently, $F(t) \sim M(t)$. The force normalized to F_m determines the load factor:

$$w = \frac{F}{F_m} = \frac{M}{M_m}, \quad w^* = \frac{F^*}{F_m} = \frac{M^*}{M_m}, \tag{10}$$

where $F_m = \Phi_r M_m$, $F^* = \Phi_r M^*$.

3. Open and internal magnetic relaxation

3.1 Time evolution of current density

The flux creep develops when the critical state is established in the superconductor; i.e. the vortex-density gradient, or induction gradient, is formed. The critical gradient determining the critical current density is established in the result of the balance of opposing forces: pinning force holding vortices on the pinning sites and Lorentz force JB which drives vortices. The form of the induction distribution is determined by the dependence of pinning force on the vortex density. We use the Bean's model of critical state according to which the vortex density is distributed in superconductor with the same gradient, i.e. the critical current density J_c = const. The greater the pinning, the larger the value J_c. Magnetic relaxation was first studied in low-temperature superconductors (LTS). The experiment shows the trapped magnetic flux gradually leaves the sample. The explanation for this phenomenon was proposed by Anderson (1962) and Anderson & Kim (1964). They introduced the concept of thermal activation. The thermal fluctuations make the vortex surmount the pinning barrier and move in the direction of the Lorentz force to the region where their density is smaller. As a result, the induction gradient and the current density decrease with time. The creep effect in LTS is so small that it almost has no effect on the characteristics of LTS devices (the current density in superconductor is close to the value J_c for a long time).

The magnetization of high-temperature superconductors decreases immediately after magnetizing. Therefore, the critical state with current density J_c is only the initial state of the magnetic structure which relaxes rapidly so that the real current density is much less than J_c. The strong magnetic relaxation can also be described by the theory of Anderson-Kim in the first approximation. The decrease of the current density starting from the moment of time t_0 may be expressed in the term of relaxation coefficient:

$$\alpha(t) = \frac{J(t > t_0)}{J_0} = 1 - \frac{kT}{U_0} \ln \frac{t}{t_0}, \tag{11}$$

where t_0 is the relaxation observation start time; $J_0 \equiv J(t_0)$; $U_0 \equiv U(t_0)$ is the effective activation energy. The magnetization and the magnetic force also change with time. The linear dependence $M(J)$ (Eq. (4)) occurs when the current flows through the whole volume of the superconductor. If the critical state does not occupy the whole volume of the sample, the dependence $M(J)$ becomes nonlinear, because r_1, r_2 and r^* in Eqs. (5) and (6) also depend on J. In this case the variation of magnetization with time depends on the location of gradient zone in the sample. As it is shown below this location determines the type of magnetic relaxation and has the considerable effect on the variation rate of magnetization and force acting on the sample.

3.2 Open magnetic relaxation

Fig. 1 (*a*) and (*b*) present the radial magnetic flux distributions established in the disk when the induction of external field changes from B_{in} (field, in which the disk was cooled) to B_s.

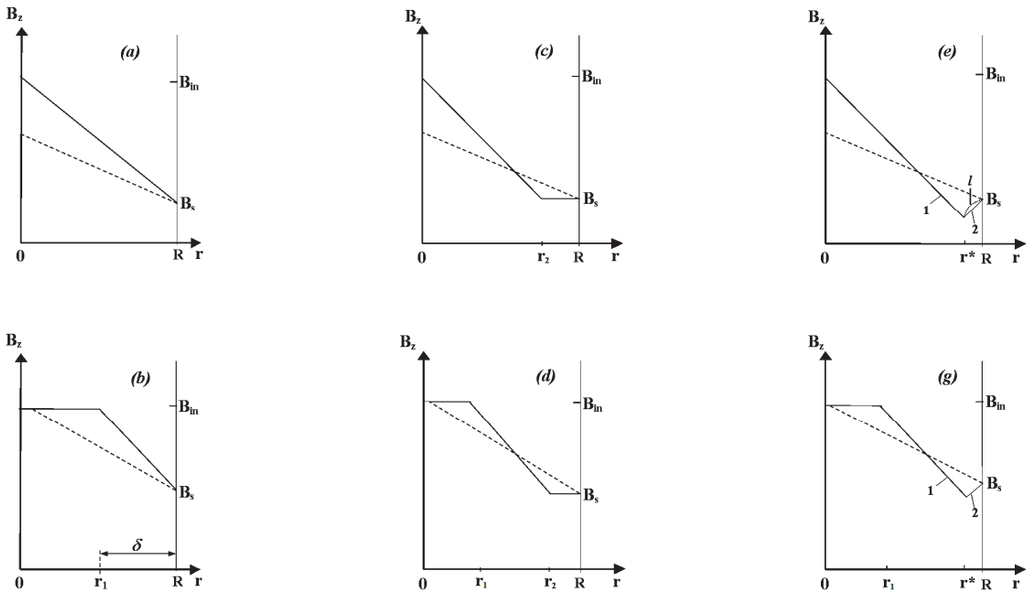

Fig. 1. One-gradient (*a*)–(*d*) and two-gradient (*e*), (*g*) magnetic flux distributions within the disk at the moment of time t' (—) and t'' (---); for all distributions $t'' \gg t'$. The time $t'' \geq t_i$ for the distributions (*c*) and (*d*); $t'' \geq t_b$ for the distributions (*e*) and (*g*).

The (*a*) and (*b*) distributions exhibit the induction gradient in the whole volume of the disk, $0 \leq r \leq R$, and the ring layer, $r_1 \leq r \leq R$, respectively. In both cases the external boundary of the critical state is located on the disk surface R through which excess of vortices leaves the sample. The flux creep related to the vortex flow through the superconductor surface will be termed *an open magnetic relaxation*. Due to the creep the distribution slope and current density decrease with the relaxation coefficient $\alpha(t)$ (Eq. (11)).

The coefficient $\beta(t) = M(t>t_0)/M(t_0)$ will be taken to characterize the magnetization relaxation. For the partial penetration (Fig. 1 (*b*)) the magnetization is determined by Eq. (5), where $r_2 = R$ and $r_1 = R - \delta(t)$; $\delta(t)$ is the penetration depth of the critical state. Considering that in the Bean's model $\delta(t) = \delta(t_0) J_0 / J(t) = \delta(t_0) / \alpha(t)$ and using Eq. (10) and relations $\delta(t_0) \equiv \delta_0$, $\hat{\delta}_0 = \delta_0 / R$, $\hat{\delta}_0 = 1 - \sqrt[3]{1 - w_0}$, and also assuming the relaxation term in Eq. (11) is small as compared to unity, one may write (here and in the sections 3.3 and 3.4 we use the results received by Smolyak et al., 2002):

$$\beta(t) = \frac{M(t > t_0)}{M_0} \cong 1 - C_\delta \frac{kT}{U_0} \ln \frac{t}{t_0}, \tag{12}$$

$$C_\delta = \frac{3\hat{\delta}_0 - 2\hat{\delta}_0^2}{3 - 3\hat{\delta}_0 + \hat{\delta}_0^2}. \tag{13}$$

For the partial penetration of the critical state, the magnetization diminishes, similarly to the current density (Eq. (11)), by a logarithmic law, but at the smaller rate, because $C_\delta<1$. If $\hat{\delta}_0 \ll 1$, then $C_\delta \cong \hat{\delta}_0 \ll 1$, i.e. the relative variation of the magnetization 1 - β(t) is much less than the change of the current density $1-\alpha(t)$. When $\hat{\delta}_0 \to 1$ (the full penetration), $C_\delta \to 1$ and $\beta(t) \to \alpha(t)$, i.e. the current density, the magnetization and the force have one and the same relaxation coefficient $\alpha(t) = J/J_0 = M/M_0 = F/F_0$.

3.3 Internal magnetic relaxation

3.3.1 Current zone removed from superconductor surface

Fig. 1 (*c*) and (*d*) present the flux distributions with the induction gradient in the region $0 \le r \le r_2$ (*c*) and $r_1 \le r \le R$ (*d*). These regions are separated from the superconductor surface R by the areas which are free of the vortex-gradient density. The induction distributions (*c*) and (*d*) may be obtained from the distributions (*a*) and (*b*) if an alternating magnetic field is applied to the latter for a short period of time. The induction gradients of the distributions (*c*) and (*d*) diminish thanks to the redistribution of vortices in the superconductor volume (We shall assume that the flux profile preserves its rectilinear behavior as in the case of distributions (*a*) and (*b*), Fig. 1). It may be shown that the current density in zone spaced from the superconductor surface has the same relaxation coefficient $\alpha(t)$ (Eq. (11)). However, oppositely to the open relaxation, the total magnetic flux remains unchanged in the sample. *An internal magnetic relaxation* takes place. The magnetization of the sample is constant, too, i.e. $\beta = M(t>t_0)/M(t_0) = 1$. The internal magnetic relaxation takes the time $t_0 \le t \le t_i$, where t_i denotes the time necessary for the emergence of boundary $r_2(t)$ on the superconductor surface R. This time may be found from Eq. (11):

$$t_i = t_0 \exp\left[(1-\alpha_i)\frac{U_0}{kT}\right], \tag{14}$$

where $\alpha_i \equiv \alpha(t_i)$ is the current relaxation coefficient at $r_2(t_i) = R$. The α_i value may be found from the condition of the full flux conservation. For the distribution in Fig. 1 (*c*) we have (considering Eq. (5), where $r_1 = 0$, and Eq. (10)):

$$\alpha_i = \left(\frac{r_{02}}{R}\right)^3 = w_0 . \tag{15}$$

For the distribution in Fig. 1 (*d*) we have:

$$\alpha_i = \frac{2\hat{\delta}_0}{3-\sqrt{4\frac{w_0}{\hat{\delta}_0}-3}}, \tag{16}$$

where $w_0 = \left(r_{02}^3 - r_{01}^3\right)/R^3$ and $\hat{\delta}_0 = \delta_0/R = (r_{02} - r_{01})/R$ (at the beginning of relaxation the size of the gradient zone $r_{02} - r_{01}$ (Fig. 1 (*d*)) is equal to the penetration depth $\delta(t_0)$ (Fig. 1 (*b*)), because the external field variation and pinning are the same in both cases).

3.3.2 Relaxation of opposite gradients

The magnetic structure with the opposite vortex-density gradients is established in the superconductor if the external field is reversed. Fig. 1 (*e*) and (*g*) present the induction distributions for the full and partial penetration of the critical state. The flux profile is a broken line comprising Sections *1* and *2*, in which the induction gradients are equal in the magnitude and opposite in the sign. The vortices diffuse during the creep to the region with the smaller vortex density, i.e. to the boundary *r** between the sections. We shall assume that the straight-line approximation is fulfilled for the both sections. Let the flux-flow density on the side of the Section *1* be larger than the density of the opposite flux flow. The excess vortices move from the Section *1* to the Section *2* and are distributed in the latter section with the same gradient as the one in the Section *1*. In another words, the Section *1* extends, while the Section *2* shrinks. (The arrangement of the gradients during the creep is similar to their rearrangement during the remagnetization of the superconductor: the new vortex distribution expands to the region with the different vortex-density gradient and "erases" the previous distribution. The only difference is that the speed of the gradient front depends on the external field variation rate in one case and on the creep velocity in another case.)

Let us consider the relaxation of distribution in Fig. 1 (*e*) when the sample has a bipolar magnetization (Eq. (6) when $r_1 = 0$). The dependences $r^*(t)$ and $M_m(t) \propto \alpha(t)$ determine the time evolution of the bipolar magnetization which proceeds with the relaxation coefficient $\beta^*(t) = M^*(t)/M_0^*$.

The bipolar magnetization is preserved in the sample for some time t_b only. Once this time has elapsed, the magnetization turns to the unipolar one and then the magnetic relaxation proceeds by the open type. It can be shown that during the time $t_0 \le t \le t_b$ the coefficient $\beta^*(t)$ changes from 1 to the value

$$\beta^*(t_b) = \frac{\alpha_b}{w_0^*} = \frac{1}{w_0^*}\left[4\sqrt{\frac{1+w_0^*}{2}} - 3\right]^{2/3}, \tag{17}$$

where $\alpha_b \equiv \alpha(t_b)$ is the current relaxation coefficient at the moment of time $t = t_b$ when the boundary r^* emerges to the superconductor surface ($r^*(t_b) = R$). Expanding Eq. (17) in the power series of $1 - w_0^*$ and keeping up to the third-order terms inclusive, we have:

$$\beta^*(t_b) \cong 1 + \frac{1}{36}\left(1 - w_0^*\right)^3, \tag{18}$$

where $w_0^* = M_0^*/M_{m0}$ is the load factor (Eq. (10)).

The relationship (17) shows that the magnetization rises slightly during the time t_b. The magnetic flux, which enters the sample during the time $t_b - t_0$, is very small. (This flux corresponds to the region limited by the initial distribution *2* and the surface *l* (see Fig. 1 (*e*)).) The lifetime of the bipolar magnetization may be calculated from Eq. (14) if t_b is substituted for t_i and α_b for α_i.

For the distribution in Fig. 1 (*g*), the relaxation pattern does not differ qualitatively from the relaxation of the distribution in Fig. 1 (*e*): the Section *1*, which contributes most to the magnetization, "swallows up" the section with the opposite magnetization. The full

magnetic flux changes little in the sample. Using the flux conservation condition and Eqs. (6) and (10), it is possible to obtain an expression for α_b which is similar in its form to Eq. (16). Here w_0 should be replaced by $w_0^* = \left(2r_0^{*3} - r_{01}^3 - R^3\right)\Big/R^3$ and $\hat{\delta}_0 = \delta_0/R = \left(2r_0^* - r_{01} - R\right)\Big/R$ (as before δ_0 is equal to the penetration depth of the critical state in Fig. 1 (*b*)).

3.4 Results of experiment and calculation

To verify the theory, we use the experimental data on the relaxation of vertical magnetic force in the "magnet-superconductor" system. The experimental setup is described in the paper of Smolyak et al. (2002). The sample of melt-textured $Yba_2Cu_3O_7$ ceramics (disk 10 mm in diameter and 3.5 mm high) and the ring magnet are used in the experiments. The sample was cooled in the initial position in the field of magnet and then was moved to the suspension point in the forward or reverse stroke. During the forward stroke from the initial position to the suspension point the sample was magnetized by the current of one polarity (unipolar magnetization). During the reverse stroke (when the sample passed the suspension point, went a certain distance (reverse depth), and then returned to the suspension point), the opposite currents passed in the sample (bipolar magnetization). The magnetic force *F*, which was acting on the HTS sample in the suspension point, was measured as a function of time. The position of the sample at this point was fixed, i.e. the magnetized sample did not move relative to the magnet when the magnetic force was changing due to the flux creep. The loaded sample, or the suspension, with total weight *G*>*F* stood on the rest all the time except the measurement moments of the force *F* (the force *P* balancing the force difference *G* – *F* was applied to the suspension for a short time and the moment of separation of suspension from the rest was recorded). The initial force F_0 was measured after t_0 = 10 min (t_0 is the time elapsed from the moment the sample was placed at the suspension point).

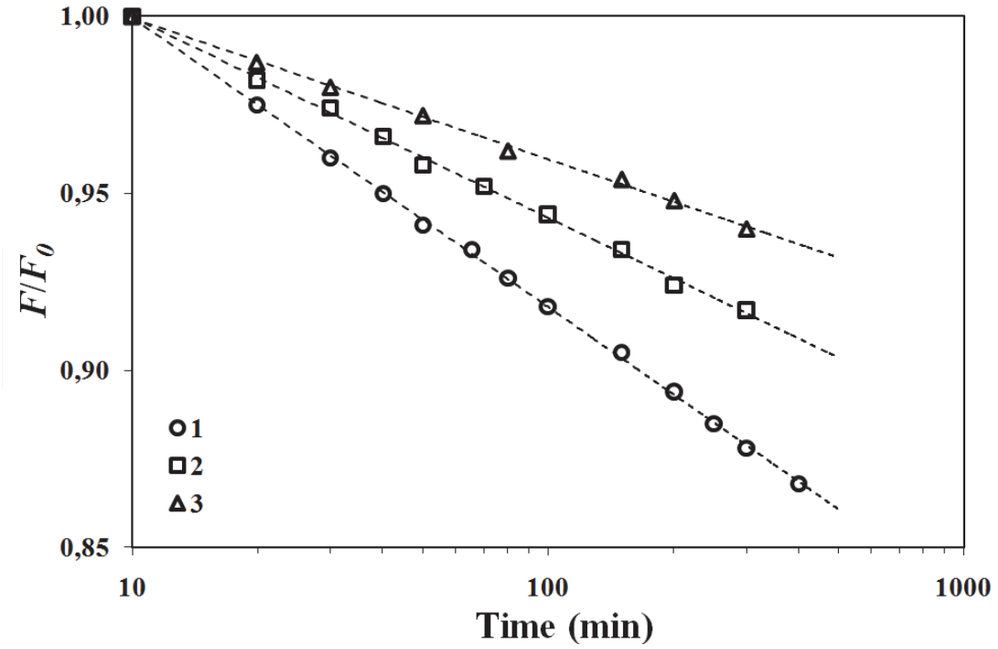

Fig. 2. Normalized magnetic force vs. time for the unipolar magnetization (open magnetic relaxation) at the different penetration depth of critical state: the initial force F_0 = 260 mN (dependence *1*), 205 mN (*2*) and 150 mN (*3*).

Fig. 2 presents the magnetic force vs. logarithmic time for the unipolar magnetization. The dependences *1-3* show the relative change of the force during the open magnetic relaxation (the flux distribution in Fig. 1 (*b*)) for different penetration depth of the critical state. These dependences also show the relative change of the sample magnetization because $F \propto M$. The slope of the dependences characterizes the logarithmic relaxation rate:

$$S_\beta = \frac{1}{F_0}\frac{dF}{d\ln t} = \frac{1}{M_0}\frac{dM}{d\ln t} = \frac{d\beta}{d\ln t}. \tag{19}$$

In the case of full penetration, the magnetization and the current-density relaxation coefficients are equal: $\beta(t) = a(t)$. From Eqs. (11) and (19) it follows that the quantity, which is inverse to the logarithmic relaxation rate, is the kT-normalized effective activation energy. In the case of partial penetration $\beta(t)$ is determined by Eq. (12). The activation energy is related to S_β as:

$$\frac{U_0}{kT} = \frac{C_\delta}{S_\beta}, \tag{20}$$

where C_δ is a correction factor (Eq. (13)). Considering open and internal magnetic relaxation we have made the assumption that the size and the location of current zone in the sample had no affect on the relaxation rate of current density. But the value of magnetization and the rate of its relaxation S_β depend on them. As follows from Eq. (20) the quantity C_δ/S_β should also be independent from the penetration depth of the critical state. The normalized penetration depth (calculated from expression $\hat{\delta} = 1 - \sqrt[3]{1 - w_0}$, where $w_0 = F_0/F_{m0}$) is equal to $\hat{\delta}_0 = 0.5$, 0.3, 0.2 at F_0 = 260, 205 and 150 mN respectively and $F_{m0} = 300$ mN. Calculating C_δ from Eq. (13) and determining the slopes S_β of the dependences *1-3* (Fig. 2), one may find that the effective activation energies are nearly equal, $U_0 \sim 15\ kT$, for all the three dependences.

However, the obtained values C_δ/S_β are very rough estimate of the effective activation energy. To calculate δ_0 and C_δ, we used the Bean's model which apparently could not describe correctly the expansion process of the critical state in the central region, i.e. for large δ_0. (The experiment shows that for $w_0 > 0.85$ the slopes of the relaxation dependences differ little from the slope of the dependence for the maximum magnetization ($w_0 = 1$). Therefore, the values δ_0/R and C_δ should be close to unity for the load coefficients, $0.85 < w_0 \le 1$.)

Fig. 3 presents the time dependence of the magnetic force for the bipolar magnetization which is imparted to the sample during the reverse stroke from the initial position to the suspension point. The force F^* is normalized to F_0 which acts at the same suspension point after the forward movement. The value of the force $F^*(t_0)$ depends on the reversal depth and, consequently, F_0^*/F_0 has different initial values (Fig. 3). The main specific feature of the dependences *1-3* consists in the presence of a plateau: the force relaxation is absent during a certain period of time. The stabilization time (the plateau) increases exponentially with the reversal depth (i.e. with decreasing F_0^*/F_0). The plateau is bounded by the dependence *4* which characterizes the relaxation of the force F acting at the same suspension point when the sample is magnetized without reversal. As soon as the force F^* reaches the said time boundary, it begins diminishing at the same rate as the force F: $dF^*/d\ln t = dF/d\ln t$.

The observed effect is described quite adequately in the terms of theory of the internal magnetic relaxation. A near-surface layer (a reverse-layer) with an opposite induction

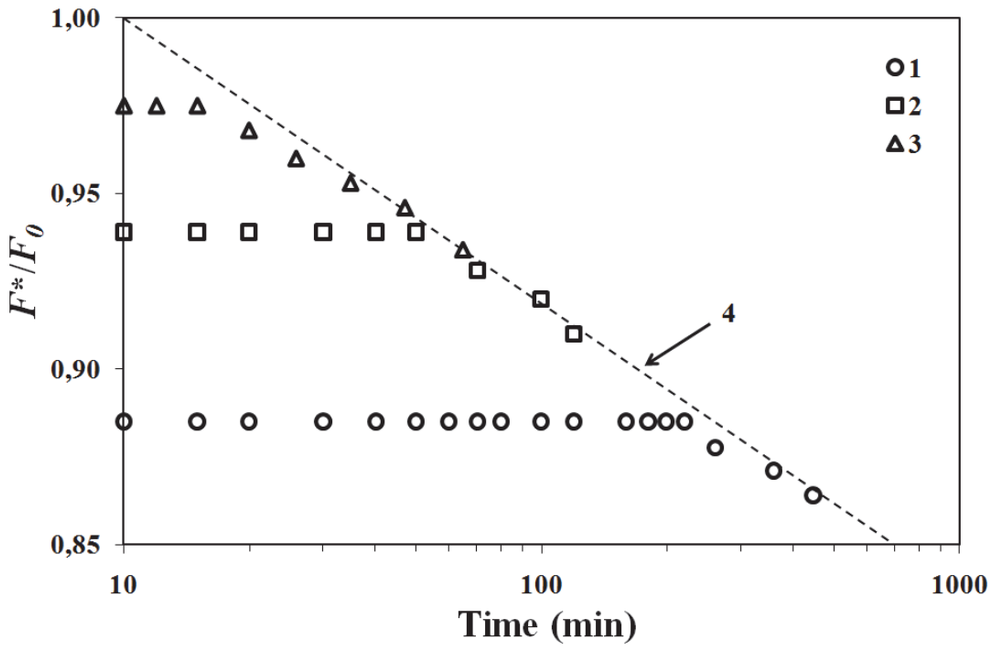

Fig. 3. Normalized magnetic force vs. time for the bipolar magnetization (internal magnetic relaxation) at the different depth of reveral: the initial force $F_0^* = 230$ mN (dependence *1*), 245 mN (*2*) and 255 mN (*3*); F_0 = 260 mN. The dashed line *4* is the approximation of data *1* in Fig. 2.

gradient appears in magnetized superconductor as a result of the small reversal of the external magnetic field. When a two-gradient distribution (Fig. 1 (*e*) and (*g*)) is relaxed, the vortices emerge from the volume to the reverse-layer rather than to the superconductor surface. The magnetic flux is redistributed inside the sample. It is known that a full force, which acts on a system of the closed-circuit currents in the magnetic field, can be expressed as the tensions operating at the boundary of the volume passing the currents. In another words, the force depends on the state of the field on the surface of the sample. Since the field does not change its state at the superconductor boundary during the time t_b , the force remains constant. The magnetic flux entering the reverse-layer on the side of the superconductor surface is very small. A relative change of the magnetization during the time t_b (the reverse-layer lifetime) is $1-\beta_b^* = -\left(1-w_0^*\right)^3 \Big/ 36$ (see Eq. (18)). In the experiment (Fig. 3) the load coefficient was $0.76 < w_0^* < 1$ which gives $\left|1-\beta_b^*\right| < 4\times 10^{-4}$. If $F_0^* \cong 250$ mN, the force variation $F_0^* - F^*\left(t_b\right) = \left(1-\beta_b^*\right)F_0^*$ is less than 0.1 mN which is beyond the sensitivity limit of the experimental installation.

Let us estimate the time t_b taking into account that the critical state does not occupy the whole volume of the disk. For the partial penetration of the bipolar critical state (Fig. 1 (g)) the current relaxation coefficient at $t = t_b$ may be calculated using the expression $\alpha_b = 2\delta_0 \Big/ \left(3-\left(4\left(w_0^*/\hat{\delta}_0\right)-3\right)^{1/2}\right)$. In experiment (Fig. 3) the normalized penetration depth

$\hat{\delta}_0 = 0.5$. The load coefficient $w_0^* = 0.766$ (for the dependence *1*), 0.816 (*2*) and 0.95 (*3*). Given these w_0^* and $\hat{\delta}_0$ values, the aforementioned formula yields $\alpha_b = 0.813$ (*1*), 0.89 (*2*) and 0.95 (*3*). The time t_b may be estimated from Eq. (14) (if α_b is substituted for α_i and t_b for t_i). If U_0/kT = 15 and t_0 = 10 min, the calculated t_b is equal to 165 min (for the dependence *1*), 50 min (*2*) and 20 min (*3*). These values approach rather closely the values observed in the experiment (Fig. 3).

4. Magnetic relaxation in levitating and "fixed" superconductors

In the paper of Smolyak et al. (2006) it was noted the results of the experimental studies of magnetic force relaxation are contradictory. The direct measurements of the interaction force between magnet and superconductor (Moon et al., 1990; Riise et al., 1992; Smolyak et al., 2002) showed a considerable decrease of the force with time. However, in the experiments, where the drift of levitating HTS samples was observed, the levitation height did not change in the stationary magnetic field (Krasnyuk & Mitrofanov, 1990; Terentiev & Kuznetsov, 1992). We suggested that in the case of levitation the relaxation rate of magnetic force was much smaller than in the case of fixed position of superconductor and magnet (when the magnetic force acts on the superconductor, and the sample is fixed at the suspension point). The force stabilization in the levitation system must arise due to feedback. Let a superconductor be magnetized as it is moving to a magnet. The magnetization and the magnetic force F will increase until F balances the sample weight. Assume that the sample magnetization is maximal in the suspension point. Then the stability of the levitation is determined by the gradient function $\Phi_r(z)$ (Eq. (9)) which increases when the sample displaces from the suspension level. If the magnetization decreases due to the flux creep, the force F will also be reduced, and the sample moving slightly from the suspension level will be biased. Therefore, F will rise again and the sample will return to the level of suspension. As a result, the magnetization and the force are almost unchanged.

The feedback may be weakened (i.e. the magnetic bias reduces) by imposing the elastic mechanical constraint on the levitating sample. In this case, the relaxation rate of magnetization and force should increase. When the constraint is absolutely rigid, there is no magnetic bias, and the magnetization relaxation rate should be the largest.

In the experiments we used the same "magnet-HTS disk" system and the same method of magnetization as described in the section 3.4. The setup was upgraded to be able to measure the rate of relaxation when the sample is imposed absolutely rigid or elastic mechanical constraint with the stiffness coefficients 500 N/m or 15 N/m (the experimental details, see in the work of Smolyak et al. (2006).

Fig. *4* shows the dependences F(*lnt*) normalized to the initial force F_0 which were measured from the time t_0 = 10 min after the magnetization of the sample. The dependences are close to linear, and its slopes $S = (\mathrm{d}F/\mathrm{d}lnt)/F_0$ characterize the logarithmic relaxation rate. The rate is maximum when the sample is fixed (dependence *1*). The relaxation slows down when the mechanical constraint is "softened" (dependences *2*-*4*). The closer the suspension system to the "true" levitation, in which the sample displacement is mainly determined by the magnetic coupling, the lower the rate of relaxation force.

To make a qualitative estimate of the experimental results, let us consider the magnetic force relaxation when the force F acts on the suspension with HTS, and at the same time the mechanical constraint is imposed on it. The magnetic force may be expressed as $F = \Phi_r M$

(Eq. (7)). For definiteness, consider the suspension of the superconductor above the magnet when the sample moving to the magnet from above is magnetized. Assume the critical state penetrates into the disk from the side surface, and the current density $J = (dB_z/dr)/\mu_0$ (Eq.(1)) is the same over the whole volume of the disk. In this case, the disk has the maximum magnetization $M = JR/3$ (Eq. (4)) (the subscript m at M is omitted). If the mechanical constraint is absolutely rigid, then J, M and F decrease with time with the same relaxation coefficient $\alpha(t)$ (Eq. (11)), i.e. $M(t)/M_0 = F(t)/F_0 = J(t)/J_0 = \alpha(t)$. If the constraint is elastic, then the current relaxation and decrease of F will cause the displacement of the suspension to the magnet. The field at the superconductor boundary grows up that leads to the formation of "fresh" critical state with the higher critical current density. The induction gradient, which is being destroyed by the flux creep, is restored.

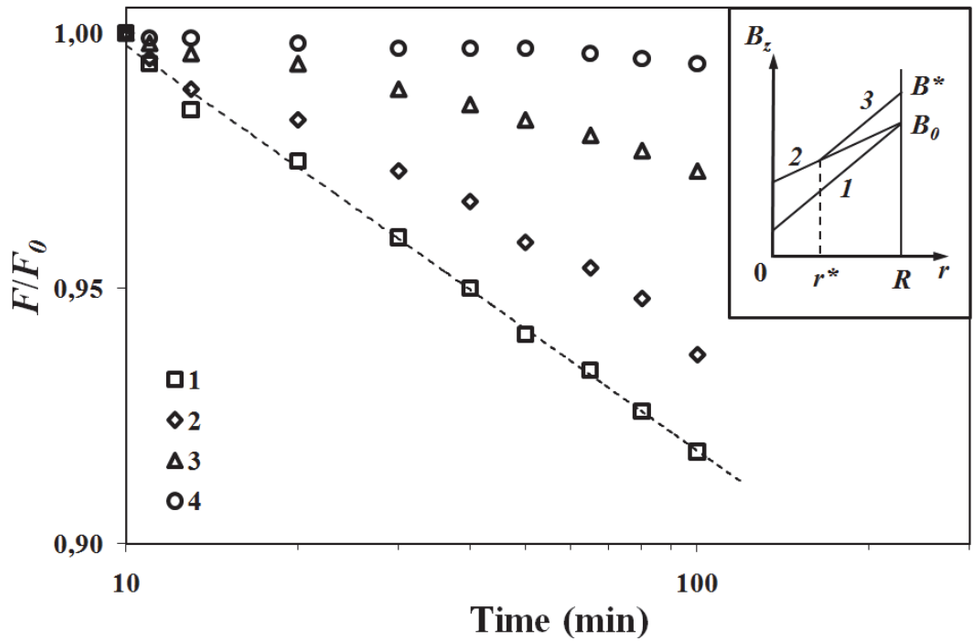

Fig. 4. The magnetic force relaxation depending on the rigidity of the constraint imposed on suspension: absolutely rigid (dependence *1*) and elastic constraint (*2*-*4*); rigidity of elastic constraint is much larger (*2*) and much smaller (*3*, *4*) than the magnetic one (suspension under (*3*) and above (*4*) the magnet). The inset shows magnetic bias process (see the text for explanation).

The inset in Fig. 4 presents the induction distribution: the initial distribution at $t = t_0$ (*1*); the distribution at $t>t_0$ in the case of rigid constraint (*2*); the distribution at the same time $t>t_0$ in the case of elastic constraint (*3*). The critical state *3* penetrates to the depth $\delta = R - r^*$. Assume that the gradient dB_z/dr in this region is restored to its initial value $\mu_0 J_0$ and, consequently, the current density is reduced only in the region $r<r^*$ where $J(t) = \alpha(t) J_0$. The disk magnetization M^* consists of two components M' and M''. Using Eq. (5), we obtain $M' = \alpha(t) M_0 \left(r^*/R\right)^3$ for region $0 \le r \le r^*$ and $M'' = M_0 \left[1 - \left(r^*/R\right)^3\right]$ for region $r^* \le r \le R$. Taking into account Eq. (11), the magnetization relaxation coefficient may be written as:

$$\beta^*(t) = \frac{M^*(t > t_0)}{M_0} = 1 - q\frac{kT}{U_0}\ln\frac{t}{t_0}, \quad (21)$$

where $M_0 = J_0R/3$, $q = [1 - (\delta/R)]^3$ is the factor of creep retardation. Assuming the function Φ_r in Eq. (7) varies slightly with the sample displacement, we have $F^*(t > t_0)/F_0 = \beta^*(t)$. The logarithmic relaxation rate $S^* = qkT/U_0$. Depending on the rigidity of mechanical constraint the factor q can range from unity ("fixed" superconductor) to zero (levitation). Using Eqs. (11) and (21) and relations $\delta = \Delta B_z/\mu_0 R(1-\alpha(t))$, $\Delta B_z = K_B\Delta z$, $\Delta z = \Delta P_m/k_m$, $\Delta P_m = \Delta F(1-\alpha(t))$ (where Δz is the suspension displacement, ΔB_z is the field variation on the boundary $r = R$, $K_B = dB_z/dz$ is the field gradient on the boundary, ΔF and ΔP_m are the variations of magnetic force and elastic mechanical force, k_m is the rigidity of mechanical constraint), the retardation factor q may be estimated from equation $Cq + q^{1/3} - 1 = 0$ where $C = F_0K_B/\mu_0k_mRJ_0$. Using $F_0 = 0.3$ N, K_B = 0.35 T/m, $J_0 = 2\times10^7$ A/m², $R = 5\times10^{-3}$ m and rigidity $k_m = \infty$, 500 N/m and 15 N/m, the calculations yield the corresponding values of q = 1, 0.705 and 0.11, respectively.

From the experiment the values of q will be found by using the dependences *1-4* (Fig. 4). The slope of the dependence *1* determines the logarithmic relaxation rate in the absence of sample displacement, i.e. factor $q = 1$. Using this condition, we obtain the kT-normalized activation energy $U_0/kT \cong 29$. The dependences *2-4* show retarded relaxation with the rate $S^* = qkT/U_0$, which yields $q = 0.724$ (the suspension under the magnet with k_m = 500 N/m), $q = 0.31$ and 0.074 (the suspension under and above the magnet, respectively, with k_m = 15 N/m). The qualitative agreement between experimental and calculated results for the factor q is quite acceptable. The magnetic relaxation slows down when the suspension system is close to the "true" levitation, i.e. when the magnetic rigidity dF/dz is much greater than the rigidity of mechanical constraint (magnetic rigidity of the "magnet-superconductor" system was ~ 100 N/m). The different values S^*, when the suspension is under (dependence *3* (Fig.4)) and above (dependence *4*) the magnet, are probably due to the different values of magnetic rigidity which determines the sample displacement if k_m is small.

Fig. 5 illustrates the effect of retarded relaxation of the magnetic force F when the superconductor levitates. Image *1* in Fig. 5 presents two identical "magnet-loaded HTS sample" systems in the initial state when the samples are on the rest above the magnet, and the force F is absent (the supporting force is not shown). When the rest goes down, and the HTS sample approaches to the magnet, the magnetic force F appears and increases until it balances the body weight G at the suspension level. In the image *2* on the left the HTS sample levitates (the rest is removed), and on the right the HTS sample remains on the rest. This image corresponds to the initial moment $t = t_0$ that has passed since the establishing of $F = G$. The image *3* shows the same position as the image *2*, but for the moment $t \gg t_0$. During this time, the levitation height on the left remains the same since the force F has not changed. On the right the force F has decreased as a result of the magnetic relaxation. The image *4* shows the positions of the HTS samples after elimination of the right rest. The right HTS sample also levitates, but its levitation height is less than the left one. (The force F, which decreased as a result of flux creep, should increase again up to the magnitude G; the HTS sample should be biased, i.e. it should go down closer to the magnet.)

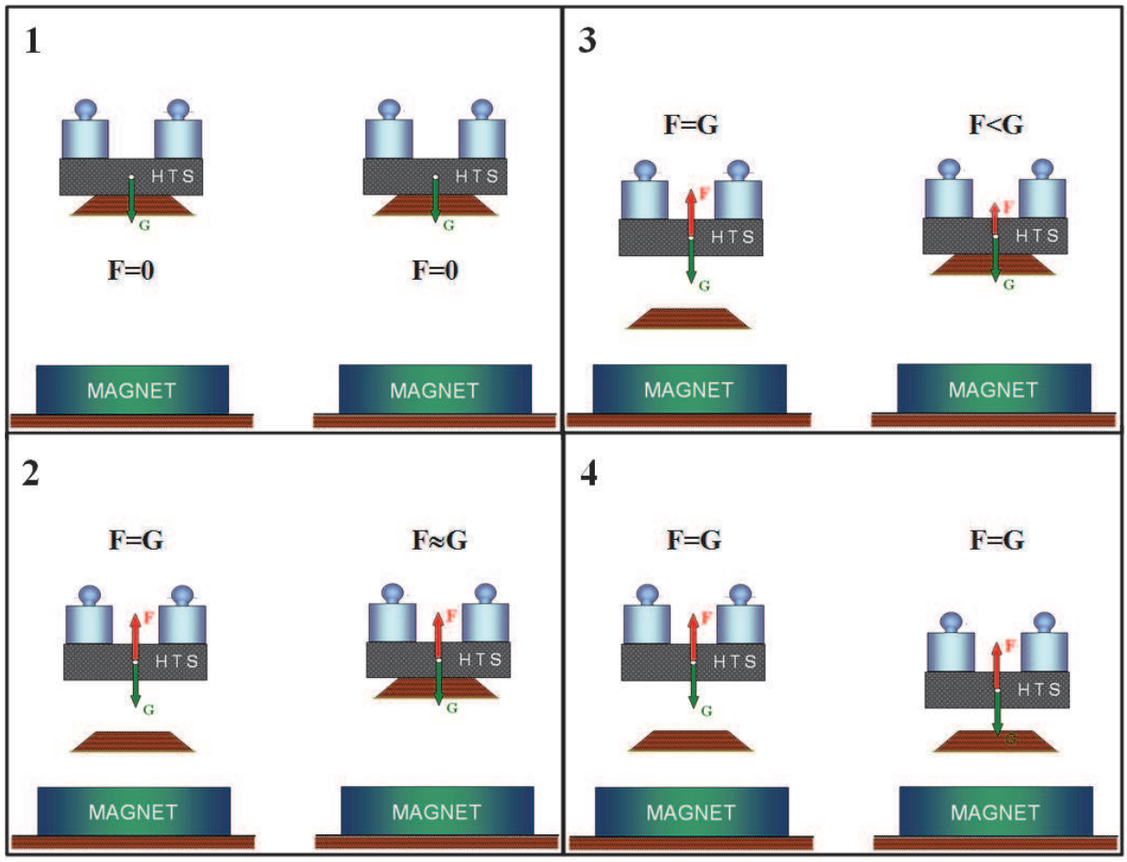

Fig. 5. The effect of retarded relaxation of the magnetic force in levitating superconductor.

5. Magnetic relaxation in superconductor placed near ferromagnet

A new effect was described by Smolyak & Ermakov (2010a, 2010b). It was found the magnetic relaxation is suppressed in HTS sample with a trapped magnetic flux when the sample approaches a ferromagnet. To have more precise idea of the conditions under which the suppression of relaxation is observed, we give a more detailed description of the experiment here.

5.1 Experimental details and results

The measurements were performed on a sample of melt-textured $YBa_2Cu_3O_7$ ceramics having the transition temperature $T_c \cong 91$ K and the transition width of less than 1 K. The sample was shaped as a disk 20 mm in diameter and 8.5 mm high. The *c*-axis was perpendicular to the disk plane. The Hall probes having the sensitive zone 1.5×0.5 mm² in size and the sensitivity of 130 μV/mT were attached to the base of the sample as sketched in the inset in Fig. 7. The probes detected the field component normal to the surface of the sample. The induction B, which determines the density of Abrikosov vortices, was measured simultaneously at five points on the surface of the sample as a function of time. (The vortices in Fig. 6 are shown conditionally as straight lines in the section of the sample. The arrow lines denote the magnetic field outside the superconductor.) The external magnetic field of the induction B_e was created by an electromagnet. Armco-iron plates (40

mm in diameter and 4 mm thick; the gap between the plates for placement of the sample was 10 mm) were also used in the experiments.

The experimental procedure was as follows. Three independent experiments on measurements of the local relaxation of the trapped magnetic flux were performed. Fig. 6 illustrates the magnetization conditions and the relative positions of the sample and the ferromagnet.

The experiment a. The HTS sample having the temperature $T>T_c$ was cooled in the external magnetic field B_e to 77 K, and then the field B_e was switched off. As a result, the sample trapped the magnetic flux (was magnetized).

The experiment b. The sample having the temperature $T>T_c$ was placed in the gap between the plates, and the external field B_e was applied to the "sample-ferromagnet" system. Then the sample was cooled, and the external field was turned off. In this experiment the sample trapped the magnetic flux when the sample and the ferromagnet were close together.

The experiment c. The sample was cooled in the field B_e, the external field was turned off, and then the sample was placed in the gap between the ferromagnetic plates. The final positions in the experiments *b* and *c* look identical, but in the experiment *b* the sample was magnetized in the presence of the ferromagnet, while in the experiment *c* the sample was first magnetized without the ferromagnet and then was brought close to it.

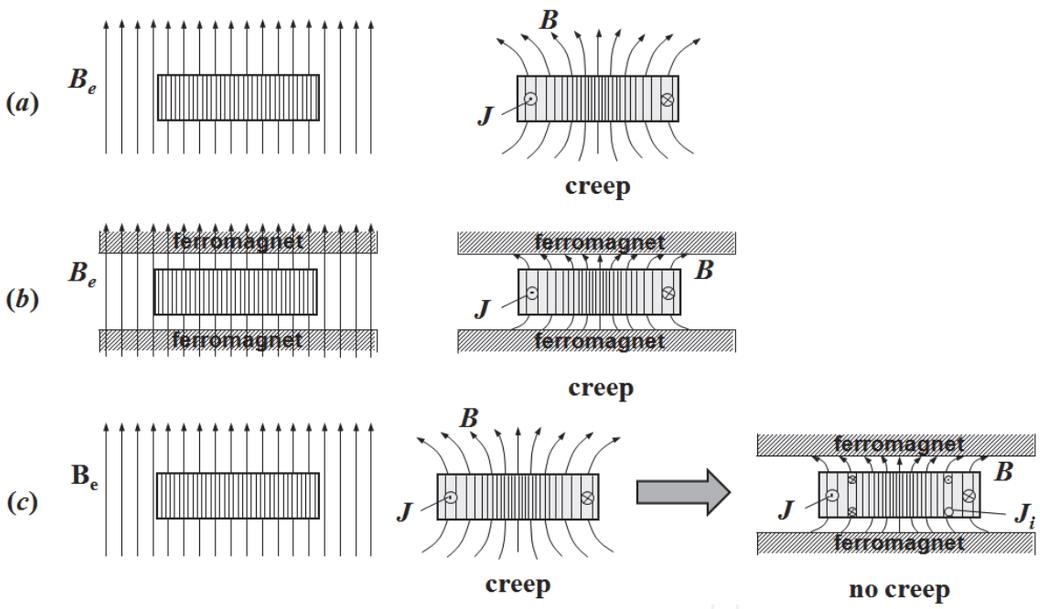

Fig. 6. Magnetizing conditions and relative position of the sample and the ferromagnet in the experiments (*a*), (*b*) and (*c*) (description of the experiments see the text). B_e , the external magnetic field; *B*, the induction of the trapped magnetic flux; *J* and J_i , the density of currents induced in the sample upon trapping of the flux and screening of the ferromagnet field, respectively.

5.2 Discussion

Fig. 7 depicts the profiles of the field which was trapped in the sample. The induction distributions on the surface of the sample was measured 2 min (the observation start point) and 100 min after the sample has been installed in the final position in the experiments *a*, *b*

or *c*. The magnetic flux in the sample decreases in the experiments *a* and *b*. The flux value remains unchanged in the experiment *c*. The form of the distributions (the absence of the plateau) suggests that the critical state occupies the whole volume of the sample.
In the absence of the ferromagnet, experiment *a*, the induction near the edge reverses sign. (This feature was also observed in the experiments with slabs in perpendicular field by Abulafia et al. (1995) and Fisher et al. (2005)).
Fig. 8 presents the normalized induction at the center of the sample versus the logarithm of time. These dependences are linear, being a characteristic feature of the flux creep. The similar dependences with sharply different relaxation rates in the experiments *a*-*c* are observed for other regions of the sample.

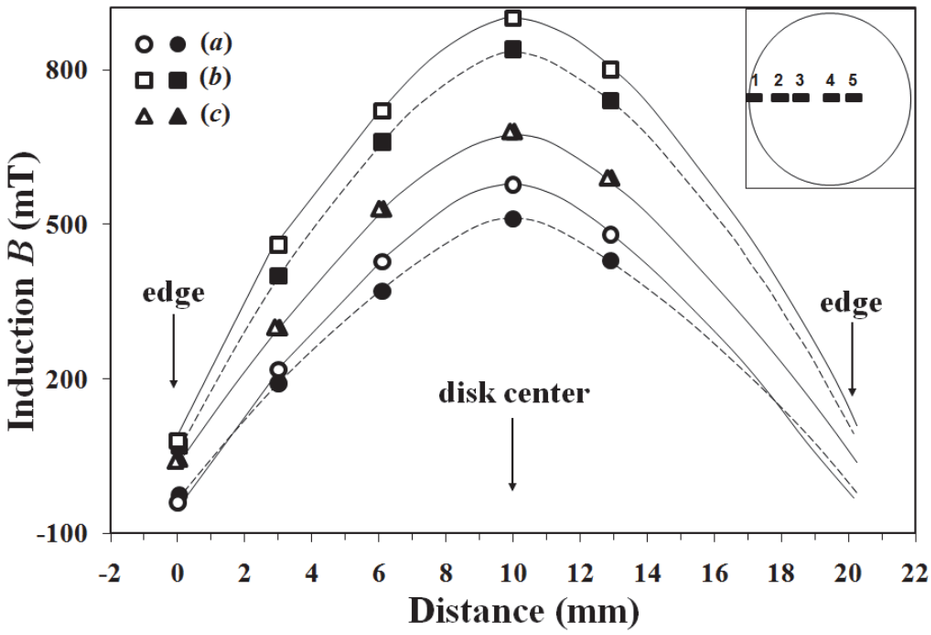

Fig. 7. Local induction *B* vs. Hall probe location measured on the surface of the sample in the experiments (*a*), (*b*) and (*c*): 2 min (open symbols) and 100 min (full symbols) after placing the sample in the final position. The solid and dashed lines serve as a guide for the eye. The inset shows the location of Hall probes.

The magnetic relaxation in the experiment *a* occurs in the absence of external effects on pinning and the nonequilibrium magnetic structure. Let us refer this relaxation to as "free". On the assumption that the current density is the same over the whole volume and diminishes at an equal rate everywhere, the local induction *B* is proportional to *J*. Therefore, the quantity $B(t)/B_0$ changes over time with the relaxation coefficient $\alpha(t)$ (Eq. (11)). The slope of the *a*-dependence, which determines the logarithmic relaxation rate, gives $1/S \sim 30$. This value is in agreement with known values of U_0/kT for melt-textured YbaCuO ceramics.
The ferromagnet retards the flux creep in the superconductor. The magnitude of the retardation effect depends on the sequence of magnetization and approach of superconductor and ferromagnet. If they are brought close together before magnetization of the superconductor (experiment *b*, Fig. 6), the relaxation rate *S* is two times lower (*b*-dependence, Fig. 8) than the "free" relaxation rate (*a*-dependence). If they are brought close

together after magnetization (experiment *c*), the magnetic relaxation is almost fully suppressed (*c*-dependence).

This effect can be interpreted as follows. The driving force $f = JB$ depends on the magnetic field configuration, which determines the value and the direction of the current in the sample. When the field at the boundary increases, i.e. the magnetic flux enters the sample, the vortex density is larger near the boundary than in the bulk, and *f* acts on the vortices in the direction from the surface to the bulk of the sample. When the field at the boundary decreases (e.g. in the case of flux trapping), the vortex density gradient is directed from the bulk to the surface, and the driving force acts in the same direction.

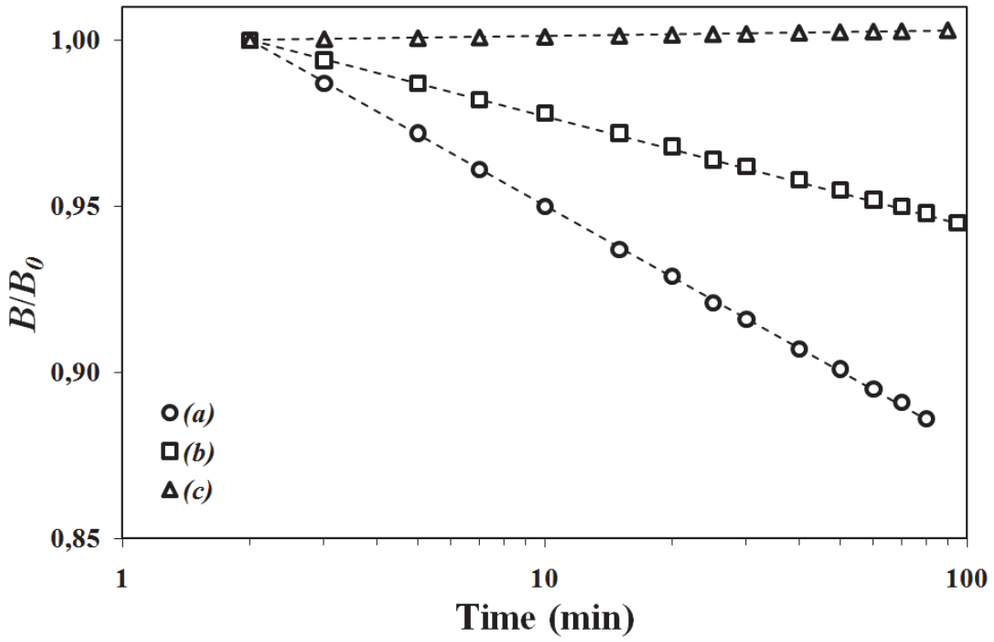

Fig. 8. Time dependence of the induction at the center of the sample normalized to the initial induction B_0 = 605 mT (experiment (*a*)), 867 mT (*b*) and 624 mT (*c*); t_0 = 2 min.

The azimuthal currents are induced in the disk sample located in the axial field. Depending on the way the external field changes upon magnetization of the sample, the critical state with forward, reverse, or counter circulation of currents is established. The magnetic field configuration, which is formed in the homogeneous external field in the absence of the ferromagnet, was calculated by Brandt (1996, 1998). The calculated configuration of the field and the direction of driving forces are shown in Fig. 9 on the left. "Free" magnetic relaxation corresponds to such direction of forces (experiment (*a*)). The current circulates in one direction in the whole volume of the sample. The driving force has two components. The radial force makes the vortices move from the center to the disk rim. The axial forces have the counter direction and do not contribute to the total force which moves vortices.

There are more complicated configurations of the flux lines in the experiments (*b*) and (*c*) because the magnetic field is produced by a screening current in the disk and by the ferromagnet. The sources of the ferromagnet field are domains oriented at the right angle to the plane of the disk. The distribution density of these domains in the disk plane

corresponds to the distribution of the local induction (Fig. 7). The ferromagnet field has the similar dome-shaped profile and has the same direction as the screening current field.
The critical state in the sample (experiment (*b*)) was established when the current in the electromagnet coil was cut off. In this case, the magnetization of the ferromagnet decreased (i.e. the number of oriented domains was reduced) from a maximum to a value corresponding to the distribution of the induction in final position in the experiment (*b*). The magnetic flux (produced by the coil and the domains, which were disorientated after the coil cutoff) left the sample through the base and the rim of the disk. As a result, the screening current circulating in one direction was excited in the sample. This state with unipolar current should undergo the magnetic relaxation. A slowdown of the creep rate in the experiment (*b*) with respect to the "free" relaxation can be due to an increase in the length of the vortices and their curvature. The effect of these factors on the total pinning force is discussed by Fisher et al. (2005) and Voloshin et al. (2007). Most likely, the mechanism of "external" pinning, which is connected with the interaction between vortices and the ferromagnetic domain structure (Garcia-Santiago et al., 2000; Helseth et al., 2002), is less probable. This effect is observed only when the superconductor and a ferromagnet are intimately in contact with each other.

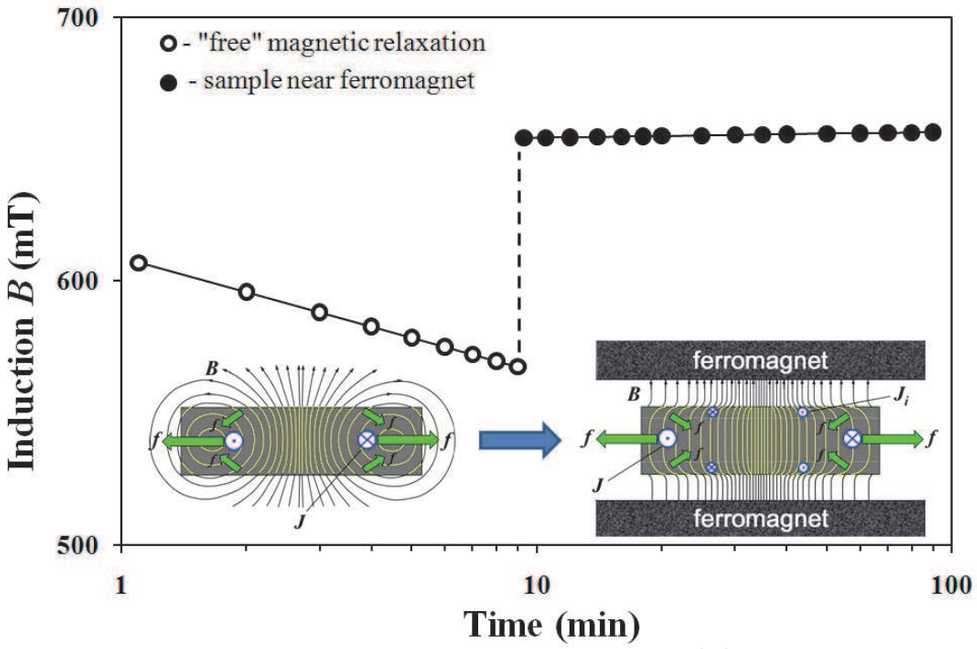

Fig. 9. The configuration of vortices and the direction of screening currents and driving forces acting on vortices, in the case of "free" magnetic relaxation (left image) and in the case the magnetized sample approaches to ferromagnet (right image). The relaxation dependences corresponding to the "free" magnetic relaxation and to the relaxation near ferromagnet are shown on the top.

The critical state in the experiment (*c*) was established when the sample with the trapped flux was placed between the ferromagnet surfaces; i.e. when the ferromagnet was brought into the magnetic field of the superconductor. Being magnetized, the ferromagnet produces its own magnetic field which penetrates into the sample and excites the currents circulating

counter to the trapping current. It can be thought that the vortex density gradients, which are connected with the ferromagnetic field, generally appear on the plane surfaces of the disk; i.e. the reverse currents flow near the base of the disk. As a result, the critical state with a bipolar current structure is established in the sample (Fig. 9, on the right). This vortex configuration is more stable because the counter driving forces *f* act on the different sections of vortices. The ferromagnet field "supports" the nonequilibrium distribution of the trapped flux, leading to the formation of a "rigid" configuration of the magnetic field which remains unchanged with time (*c*-distribution, Fig. 7).

6. Conclusion

We have been considered the influence of the conditions of magnetization, the mobility of the samples in magnetic suspension system and the ferromagnetic medium on the relaxation rate of magnetization and magnetic force in bulk high-temperature superconductors.

(i) The features of open and internal magnetic relaxation have been discussed. It has been shown that both strong decrease in magnetization and force (open relaxation) and absence of any changes of these parameters (internal relaxation) could be observed in experiment. The magnetization of the sample and the magnetic force are stabilized thanks to the reversal of external magnetic field. A model is proposed for the internal magnetic relaxation which arises when the nonequilibrium region of vortex lattice is far from superconductor surface or is separated from it by the layer with an opposite vortex-density gradient.

(ii) It has been shown that in a "magnet-superconductor" system the creep rate depends on the rigidity of the constraints imposed on the system. The magnetization of the superconductor and the magnetic force decrease at a maximum rate when the HTS sample and the magnet are rigidly fixed. In the case of "true" levitation (when the mobility of the sample is determined predominantly by magnetic coupling) the magnetic force very slightly decreases with time. It is suggested that the force stabilization is related to magnetic bias feedback in the sample which restores the nonequilibrium structure broken by the magnetic flux creep.

(iii) It has been described the phenomenon of the retardation of magnetic relaxation in the HTS sample with a trapped magnetic flux when the sample approached a ferromagnet. The flux creep is fully suppressed when the superconducting sample first is magnetized and then the ferromagnet is brought into the magnetic field of the superconductor. It is supposed that the phenomenon results from the formation of stable vortex configuration in which counter Lorentz forces act upon the different regions of vortices.

7. References

Abulafia, Y.; Shaulov, A.; Wolfus, Y.; Prozorov, R.; Burlachkov, L.; Yeshurun, Y.; Majer, D.; Zeldov, E. & Vinokur, V.M. (1995). Local magnetic relaxation in high-temperature superconductors. *Phys. Rev. Lett.*, Vol.75, No.12, (September 1995), pp. 2404-2407, ISSN 0031-9007

Anderson, P.W. (1962). Theory of flux creep in hard superconductors. *Phys. Rev. Lett.*, Vol.9, No.7, (October 1962), pp. 309-311, ISSN 0031-9007

Anderson, P.W. & Kim, Y.B. (1964). Hard superconductivity: theory of the motion of Abrikosov flux lines. *Rev. Mod. Phys.*, Vol.36, No.1, (January 1964), pp. 39-43, ISSN 0034-6861

Beasly, M.R.; Labusch, R. & Webb, W.W. (1969). Flux creep in type-II superconductors. *Phys. Rev.*, Vol.181, No.2, (May 1969), pp. 682-700, ISSN 0143-0394

Brandt, E.H. (1996). Superconductors of finite thickness in a perpendicular magnetic field: strips and slabs. *Phys. Rev. B*, Vol.54, No.6, (August 1996), pp. 4246-4264, ISSN 1098-0121

Brandt, E.H. (1998). Superconductor disk and cylinders in an axial magnetic field. I. Flux penetration and magnetization curves. *Phys. Rev. B*, Vol.58, No.10, (September 1998), pp. 6506-6522, ISSN 1098-0121

Brandt, E.H. & Mikitik, G.P. (2003). Reversible magnetic behavior of superconductors forced by a small transverse ac magnetic field. *Journal of Low Temperature Physics*, Vol.131, No.5-6, (June 2003), pp. 1033-1042, ISSN 0022-2291

Fisher, L.M.; Kalinov, A.V.; Voloshin, I.F. & Yampol'skii, V.A. (2005). Suppression of magnetic relaxation processes in melt-textured $YBa_2Cu_3O_x$ superconductors by a transverse ac magnetic field. *Phys. Rev. B*, Vol.71, No.14, (April 2005), pp. 140503-(1-4), ISSN 1098-0121

Fisher, L.M.; Kalinov, A.V.; Savel'ev, S.E.; Voloshin, I.F.; Yampol'skii, V.A.; LeBlanc, M.A.R. & Hirscher, S. (1997). Collapse of the magnetic moment in a hard superconductor under the action of a transverse ac magnetic field. *Physica C*, Vol.278, No.3-4, (May 1997), pp. 169-179, ISSN 0921-4534

Garcia-Santiago, A.; Sanchez, F.; Varela, M. & Tejada, J. (2000). Enhanced pinning in a magnetic-superconducting bilayer. *Appl. Phys. Lett.*, Vol.77, No.18, (December 2000), pp. 2900-2902, ISSN 0003-6951

Helseth, L.E.; Goa, P.E., Hauglin, H.; Baziljevich, M. & Johansen, T.H. (2002). Interaction between a magnetic domain wall and a superconductor. *Phys. Rev. B*, Vol.65, No.13, (March 2002), pp. 132514-(1-4), ISSN 1098-0121

Krasnyuk, N.N. & Mitrofanov, M.P. (1990). Levitation of YbaCuO ceramics in magnetic field. *Superconductivity: Physics, chemistry, technique*, Vol.3, No.2, (February 1990), pp. 318-322, ISSN 0131-5366

Kwasnitza, K. & Widmer, Ch. (1991). Strong magnetic history dependence of magnetic relaxation in high-T_c superconductors. *Physica C*, Vol.184, No.4-6, (December 1991), pp. 341-352, ISSN 0921-4534

Kwasnitza, K. & Widmer, Ch. (1993). Methods for reduction of flux creep in high and low T_c type II superconductors. *Cryogenics*, Vol.33, No.3, (March 1993), pp. 378-381, ISSN 0011-2275

Landau, L.D.; Lifshitz, E.M. & Pitaevskii, L.P. (1984). *Course of theoretical physics, vol.8 – Electrodynamics of continuous media* (2nd edition), Pergamon Press, ISBN 0080302750, New York

Maley, M.P.; Willis, J.O.; Lessure, H. & McHenry, M.E. (1990). Dependence of flux-creep activation energy upon current density in grain-aligned $YBa_2Cu_3O_{7-x}$. *Phys. Rev. B*, Vol.42, No.4, (August 1990), pp. 2639-2642, ISSN 1098-0121

Moon, F.C.; Chang, P.-Z.; Hojaji, H.; Barkatt, A. & Thorpe, A.N. (1990). Levitation forces, relaxation and magnetic stiffness of melt-quenched $YBa_2Cu_3O_x$. *Japanese Journal of Applied Physics*. Vol.29, No.7, (July 1990), pp. 1257-1258, ISSN 0021-4922

Riise, A.B.; Johansen, T.H.; Bratsberg, H. & Yang, Z.J. (1992). Logarithmic relaxation in the levitation force in a magnet-high T_c superconductor system. *Appl. Phys. Lett.* Vol.60, No.18, (May 1992), pp. 2294-2296, ISSN 0003-6951

Smolyak, B.M.; Perelshtein, G.N.; Ermakov, G.V. & Postrekhin, E.V. (2000). Stopping of levitation force relaxation in superconductors: the flux-locking effect. *Physica C*, Vol.341-348, No.PART 3, (November 2000), pp. 1129-1130, ISSN 0921-4534

Smolyak, B.M.; Perelshtein, G.N. & Ermakov, G.V. (2001). Internal magnetic relaxation in levitating superconductors. *Technical Physics Letters*, Vol.27, No.8, (August 2001), pp. 674-676, ISSN 1063-7850

Smolyak, B.M.; Perelshtein, G.N. & Ermakov, G.V. (2002). Effects of relaxation in levitating superconductors. *Cryogenics*, Vol.42, No.10, (October 2002), pp. 635-644, ISSN 0011-2275

Smolyak, B.M.; Perelshtein, G.N. & Ermakov, G.V. (2006). Retarded magnetic relaxation in levitated superconductors. *Technical Physics Letters*, Vol.32, No.2, (February 2006), pp. 98-100, ISSN 1063-7850

Smolyak, B.M.; Ermakov, G.V. & Chubraeva, L.I. (2007). The effect of ac magnetic fields on the lifting power of levitating superconductors. *Superconductor Science and Technology*, Vol.20, No.4, (April 2007), pp. 406-411, ISSN 0953-2048

Smolyak, B.M. & Ermakov, G.V. (2010). Elimination of magnetic relaxation in superconductors on approaching a ferromagnet. *Physica C*, Vol.470, No.3, (February 2010), pp. 218-220, ISSN 0921-4534

Smolyak, B.M. & Ermakov, G.V. (2010). Suppression of magnetic relaxation in a high-temperature superconductor placed near a ferromagnet. *Technical Physics Letters*, Vol.36, No.5, (May 2010), pp. 461-463, ISSN 1063-7850

Sun, J.Z.; Lairson, B.; Eom, C.B.; Bravman, J. & Geballe, T.H. (1990). Elimination of current dissipation in high transition temperature superconductors. *Science*, Vol.247, No.4940, (January 1990), pp. 307-309, ISSN 0036-8075

Terentiev, A.N. & Kuznetsov, A.A. (1992). Drift of levitated YBCO superconductor induced by both a variable magnetic field and a vibration. *Physica C*, Vol.195, No.1-2, (May 1992), pp. 41-46, ISSN 0921-4534

Thompson, J.R.; Sun, Y.R.; Malozemoff, A.P.; Christen, D.K.; Kerchner, H.R.; Ossandon, J.G.; Marwick, A.D. & Holtzberg, F. (1991). Reduced flux motion via flux creep annealing in high-J_c single-crystal $Y_1Ba_2Cu_3O_7$. *Appl. Phys. Lett.*, Vol.59, No.20, (November 1991), pp. 2612-2614, ISSN 0003-6951

Voloshin, I.F.; Kalinov, A.V.; Fisher, L.M. & Yampol'skii, V.A. (2007). Suppression of magnetic relaxation by a transverse alternating magnetic field. *Journal of Experimental and Theoretical Physics*, Vol.105, No.1, (July 2007), pp. 278-282, ISSN 1063-7761

Willemin, M.; Rossel, C.; Hofer, J.; Keller, H.; Erb, A. & Walker, E. (1998). Strong shift of the irreversibility line in high-T_c superconductors upon vortex shaking with an

oscillating magnetic field. *Phys. Rev. B*, Vol.58, No.10, (September 1998), pp. R5940-R5943, ISSN 1098-0121

Yeshurun, Y.; Malozemoff, A.P. & Shaulov, A. (1996). Magnetic relaxation in high-temperature superconductors. *Rev. Mod. Phys.*, Vol.68, No.3, (July 1996), pp. 911-949, ISSN 0034-6861

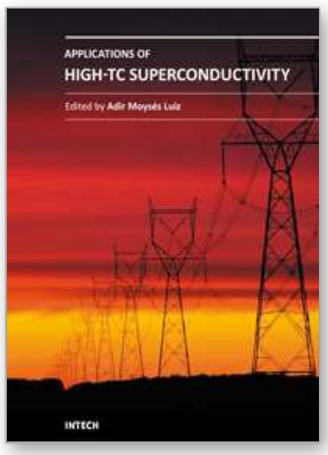

Applications of High-Tc Superconductivity
Edited by Dr. Adir Luiz

ISBN 978-953-307-308-8
Hard cover, 260 pages
Publisher InTech
Published online 27, June, 2011
Published in print edition June, 2011

This book is a collection of the chapters intended to study only practical applications of HTS materials. You will find here a great number of research on actual applications of HTS as well as possible future applications of HTS. Depending on the strength of the applied magnetic field, applications of HTS may be divided in two groups: large scale applications (large magnetic fields) and small scale applications (small magnetic fields). 12 chapters in the book are fascinating studies about large scale applications as well as small scale applications of HTS. Some chapters are presenting interesting research on the synthesis of special materials that may be useful in practical applications of HTS. There are also research about properties of high-Tc superconductors and experimental research about HTS materials with potential applications. The future of practical applications of HTS materials is very exciting. I hope that this book will be useful in the research of new radical solutions for practical applications of HTS materials and that it will encourage further experimental research of HTS materials with potential technological applications.

How to reference
In order to correctly reference this scholarly work, feel free to copy and paste the following:

Boris Smolyak, Maksim Zakharov and German Ermakov (2011). Magnetic Relaxation - Methods for Stabilization of Magnetization and Levitation Force, Applications of High-Tc Superconductivity, Dr. Adir Luiz (Ed.), ISBN: 978-953-307-308-8, InTech, Available from: http://www.intechopen.com/books/applications-of-high-tc-superconductivity/magnetic-relaxation-methods-for-stabilization-of-magnetization-and-levitation-force

INTECH
open science | open minds

InTech Europe
University Campus STeP Ri
Slavka Krautzeka 83/A
51000 Rijeka, Croatia
Phone: +385 (51) 770 447
Fax: +385 (51) 686 166
www.intechopen.com

InTech China
Unit 405, Office Block, Hotel Equatorial Shanghai
No.65, Yan An Road (West), Shanghai, 200040, China
中国上海市延安西路65号上海国际贵都大饭店办公楼405单元
Phone: +86-21-62489820
Fax: +86-21-62489821

IntechOpen